Underwater attachment in current: the role of setose attachment structures on the gills of the mayfly larvae *Epeorus assimilis* (Ephemeroptera, Heptageniidae)

P. Ditsche-Kuru[1,*], J. H. E. Koop[2] and S. N. Gorb[3,4]

[1]Biological Interfaces Working Group, Nees Institute for Biodiversity of Plants, University of Bonn, Meckenheimer Allee 170, 53115 Bonn, Germany, [2]Department of Animal Ecology, Federal Institute of Hydrology, 56068 Koblenz, Germany, [3]Evolutionary Biomaterials Group, Max Plank Institute for Metal Research, Heisenbergstrasse 3, 70569 Stuttgart, Germany and [4]Department of Functional Morphology and Biomechanics, Zoological Institute of the University of Kiel, Am Botanischen Garten 1-9, 24098 Kiel, Germany

*Author for correspondence (p.ditsche-kuru@uni-bonn.de)

SUMMARY

Setose pads of aquatic *Epeorus assimilis* larvae are specialised structures located ventrally on the part of the gill lamella contacting the substrate and were suggested to have an attachment function in strong currents. In order to test the role of these setose pads in underwater attachment for the first time, we measured friction (shear) forces generated by the gill lamellae on solid substrates. Moreover, the influence of a different kind of surface roughness on attachment was investigated. Scanning electron microscopy showed that four different seta types can be found on the pads. Our results revealed that the pads significantly contributed to friction force generated on smooth and on some rough substrates but not on certain surfaces of intermediate roughness. The contribution of pads to the friction coefficient in experiments was lower than expected under natural conditions, which may be caused by a smaller contact area between the pads and the substrate (changes in material properties, lack of the active control of body positioning of the larva). The friction coefficient of the gill lamellae with the substrate depended on the surface roughness of the substrate and on the pulling direction. These results suggest that interlocking between structures of the insect cuticle and substrate irregularities, as well as molecular adhesion, contribute to friction.

Key words: microstructure, attachment, gill lamellae, friction, setose pads, *Epeorus assimilis*.

INTRODUCTION

Larvae of the mayfly *Epeorus assimilis* Eaton 1885 (Heptageniidae) are typical grazers in swift-running waters (Minshall, 1967; Wellnitz et al., 2001). In order to graze upon algae, they crawl on the surface of stony substrates, a position that exposes them to the current. Previous authors have assumed that many running-water insects live within the reduced flow in the boundary layer at the surface of the substrate and, therefore, do not need much further adaptations to flow forces (Ambühl, 1959). However, in the meantime it was shown that macrozoobenthic organisms have to cope with noteworthy flow forces (Statzner and Holm, 1982). To withstand these forces, larvae developed a number of morphological adaptations such as dorso-ventral flattening of the body, strong claws (Fig. 1B) and strong laterally directed legs (e.g. Haybach and Malzacher, 2002).

Because larvae in strong current always orient themselves to face the flow, it was assumed that the specialised body shape and body posture of the larvae in current deflects water in such a way that one component of the drag force is used to press the animal against the substrate (Dodds and Hisaw, 1924; Gonser, 1990; Ditsche-Kuru and Koop, 2009). The gill lamellae, overlapping each other like roof tiles, resemble a suction cup and give the larva a very typical look (Fig. 1A). However, the assumption that gill lamellae of *E. assimilis* work like a sucker (e.g. Wesenberg-Lund, 1943; Ruttner, 1962; Bauernfeind and Humpesch, 2001; Staniczek, 2003) was already doubted 40 years ago (Hynes, 1970). Recently it has been shown that the gill lamellae do not form a complete seal (Ditsche-Kuru and Koop, 2009), and the following additional structures with probable attachment function have been documented: setose pads

on the ventral margins of gill lamellae and areas with spiky acanthae on abdominal sterna (Fig. 1C,D). The setose pads are located on the part of the gill lamellae that was observed in video recordings to stay in contact with the substrate even in strong currents (Ditsche-Kuru and Koop, 2009). A fringe of setae on the ventral side of the gill lamellae, labelled adhesive structures, was also shown on the scanning electron microscopy (SEM) pictures of a related *Epeorus* species (Wichard et al., 2002). However, so far, no attachment experiments were made with these aquatic setose pads. Contrary to many related species, which are able to move their gills and adjust their gill beat frequency for respiration (Eastham, 1936), the lamellae of *E. assimilis* have been previously described as immobile (e.g. Ambühl, 1959; Baeumer et al., 2000).

Conspicuously, the setose pads of gill lamellae in the lotic *E. assimilis* larvae look somewhat similar to the setose attachment pads of some terrestrial insects [e.g. *Forficula auricularia*, Dermaptera (Haas and Gorb, 2004)]. In terrestrial insects, lizards and spiders, setose or 'hairy' pads play an important role in attachment (Autumn et al., 2000; Gorb, 2001; Gorb et al., 2002; Kesel et al., 2004). They are known for their high attachment force, fast attachment/detachment ability and force directionality (Autumn, 2006). Due to the flexibility of setose surfaces the possible contact with the substrate is maximised, regardless of its microsculpture (Gorb and Beutel, 2001). Attachment force in such systems is described to be a combination of molecular interactions (van der Waals forces) and capillary attractive forces mediated by pad secretion in insects (Stork, 1980; Langer et al., 2004). In lizards, the attachment system mainly relies on van der Waals interactions (Autumn et al., 2000) but
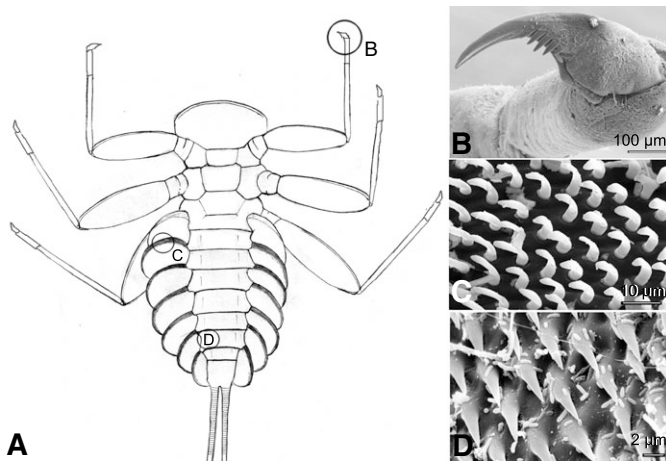
Fig. 1 Attachment devices of *Epeorus assimilis* larvae: (A) ventral view of an *E. assimilis* larva, (B) claw of the first leg, (C) setae of the pads on the ventral side of the gill lamellae, (D) areas with spiky acanthae on the lateral parts of the abdominal sternits.

wetting phenomena can additionally contribute to the generation of attractive forces (Huber et al., 2005). So far no equivalent experiments have been done on the setose pads of gill lamellae of aquatic mayfly larvae. Using light microscopy, these structures were described as spines with sharp tips for *Epeorus* sp. from the Himalaya, suggesting that they are marvellous friction pads (Hora, 1930). Kluge mentioned that the costal rib of the gill lamellae in some *Epeorus* species is covered by spine-like setae probably supporting the larva for coupling with stones (Kluge, 2004). Using SEM compressed tips were found, at least for *Epeorus assimilis* and *Iron alpicola* (Ditsche-Kuru and Koop, 2009).

Setose attachment pads from terrestrial insects are known to have an excellent ability to adhere to smooth surfaces (Gorb and Beutel, 2001). Interestingly, also for *Epeorus* species, the ability to move on smooth glass in running water has been previously mentioned (Ambühl, 1959). Furthermore, *E. assimilis* larvae were observed adhering to smooth Plexiglas surfaces (P.D.-K., unpublished). Knowing that the gill lamellae cannot function as true hydraulic suckers (Ditsche-Kuru and Koop, 2009), the question arises as to whether or not setose pads contribute to the ability of larvae to adhere to smooth surfaces. A second question concerns the role and contribution of setose pads in attaching to rough surfaces. Experiments with flies, beetles and geckos show that the roughness plays an important role in the attachment of terrestrial animals (Gorb, 2001; Dai et al., 2002; Huber et al., 2007). It was suggested that the different attachment structures of *Epeorus* larvae may provide an adaptation to underwater attachment on substrates with a different surface profile (Ditsche-Kuru and Koop, 2009). In this study, we present the first experimental results ever on the contribution of the setose pads of *E. assimilis* to attachment. Moreover, for the first time, we experimentally measured the influence of the substrate surface structure on attachment of the gill lamellae.

The objective of this study was to understand the function of setose pads on gill lamellae of *E. assimilis* in attachment. Using friction measurements, video recording and SEM the following questions were asked: (1) do the setose pads on the gill lamellae increase the friction force with the substrate? (2) Does such an effect depend on the surface roughness? (3) Is the attachment force of the setose pads of *E. assimilis* dependent on the direction of the pulling force? (4) Can the gill lamella position be controlled by the insect?

MATERIALS AND METHODS
Animals
Epeorus assimilis larvae were collected in small rivers located in the Thuringian Forest, Germany, and kindly provided by the Museum of Natural History of the city of Gotha. After collection, several larvae were transported live to the laboratory flume in a cooled box. Specimens for friction experiments were obtained in 70% ethanol.

Measurement of friction force
For friction experiments, larvae fixated in 70% ethanol and rehydrated in water for at least 3 h were used. Afterwards, all legs were cut off, and the larva was positioned on a slide with the ventral side down. Gill lamellae were dorsally fixed by means of wax drops in such a way that the ventral side of the larva and its gill lamellae have contact to the support.

The experimental design is shown in Fig. 2. The larva preparation was glued dorsally to a small glass plate by means of double-sided adhesive tape and the complete preparation was then positioned on the substrate. The substrate was mounted on the bottom of a Petri dish, which was then connected to an immobile stage and filled with tap water. The glass plate with the larva preparation was connected with a force transducer by means of a human hair. The distance between the plate and force transducer was 5.5–5.8 cm. The human hairs had to be renewed twice in the course of experiments due to damaging during the exchange of preparations. The angle between the hair and the direction of the pull was determined, in order to calculate applied forces. Friction measurements were carried out in a combination of constant movements of a motorised micromanipulator and the force monitoring using a load cell force transducer (100 g capacity, Biopac Systems Ltd, Santa Barbara, CA, USA). For this purpose, the force transducer was mounted on the micromanipulator (MS314, M/W, Märzhäuser, Wetzlar, Germany). The micromanipulator was moved in a horizontal direction with a constant velocity of $100 \, \mu m \, s^{-1}$. During movement, friction force
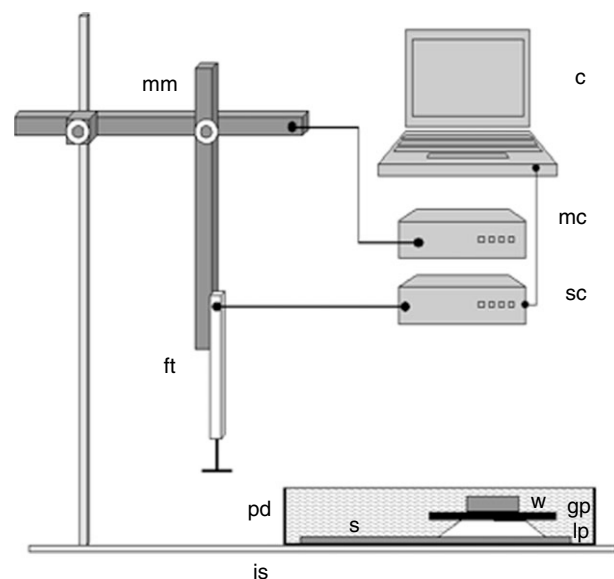

Fig. 2. Experimental design for force measurements: mm, motorised micromanipulator; ft, force transducer; c, computer; mc, motor control; sc, sensor control; is, immobile stage; w, weight; gp, glass plate; lp, larval preparation; s, substrate; pd, Petri dish.
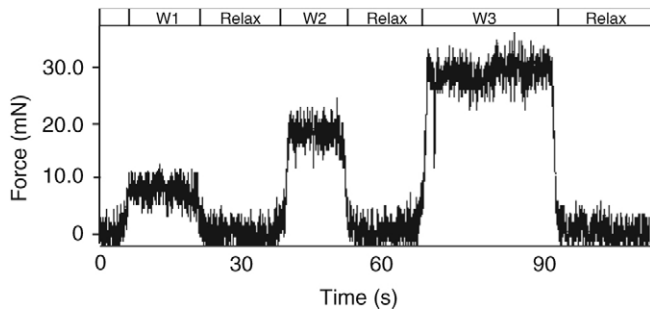
Fig. 3. Example of a typical friction force curve generated by the ventral surface of *Epeorus assimilis* under different loads (W1–W3). In relaxing phases the larval preparation was not moved while in W phases the preparation was drawn over the substrate. Friction force was measured for three different normal loads: (W1) weight of the larval preparation plus glass plate; (W2) similar to W1 with one added weight; (W3) similar to W1 with two added weights.

was monitored for different loads. Friction force (**F**) is here defined as the force that has to be overcome to move the larva over a substrate. Mean friction force was extracted after data processing (Fig. 3).

Friction force was measured for three different normal loads. Besides the larval preparation plus the small glass plate necessary for experimental design (W1), normal force (F_{normal}) was increased by one (W2) or two added weights (W3) of 2.18 g each. In contrast to terrestrial conditions, the acting normal force on *Epeorus* larvae is determined less by the weight of the animal itself but rather more by the body posture and flow conditions. Because the range of normal forces acting on the larva under real environmental conditions is not known we chose a wide range of normal forces to test frictional behaviour of setose pads under various load conditions. The normal load of different weights was determined for all preparations under water by means of the force transducer. The range of normal force was 11.9–12.6 mN for W1, 33.5–34.1 mN for W2 and 55.1–55.8 mN for W3. Furthermore, four substrate types were tested: (S1) glass as a reference for a smooth surface structure; (S2) polishing paper with a nominal asperity size of 1 μm; (S3) polishing paper with a nominal asperity size of 12 μm, and (S4) polishing paper of grain size 400 (classification according to DIN ISO 6344). The height of the water level was the same for all substrates. Measurements were made using forces acting in posterior and anterior directions on the body. Original measurements were made with larval preparations with intact gill lamellae. After removing the gill lamellae from the larval preparation, measurements were repeated for all factor combinations. For each factor combination, five larvae were measured with seven repetitions.

Determination of surface parameters

All four substrate types were measured by means of white light interferometer (FRT MicroProf, CHR 150N high resolution optical sensor, Fries Research & Technology, Bergisch Gladbach, Germany) to determine surface topography. The determination of surface roughness was made at two different magnifications in order to detect different scales of surface roughness. At the lower magnification an area of 1000 μm×1000 μm (pixel size: 10 μm^2) was measured whereas at higher magnification an area of 100 μm×100 μm (pixel size: 1 μm^2) was scanned. Each substrate and magnification was measured in 10 different areas on the

substrate surface. 3-D profiles and analyses of roughness parameters were made using FRT-Mark III software. For comparison of the substrates two common roughness parameters were selected: the arithmetic roughness mean (R_a) and the mean maximum height of the profile (R_z). R_a is the arithmetic mean of the absolute values of the roughness profile ordinates whereas R_z is the mean distance between the highest peak and the lowest valley in each sampling length. The cutoff length (λ_c) defines the limit between roughness and waviness and therefore influences the values of the roughness parameters. According to Volk, the length of λ_c was defined as one-sixth of the length of the measured profiles (Volk, 2005). Therefore, the cutoff length was 166.7 μm in the lower magnification setting and 16.7 μm in the higher magnification setting.

Gill movement experiments

Gill movement experiments were performed in a laboratory flume described in detail in a preceding study (Ditsche-Kuru and Koop, 2009). In the flume, larvae were recorded by means of a videoscope (Iplex II, Olympus, Hamburg, Germany, 25 frames s^{-1}). Selected video sequences were evaluated and digitised into single pictures using SIS image processing software EIS (Olympus, Münster, Germany). Larvae attached to a Plexiglas plate inside the flume were video recorded from the ventral side in order to observe attachment of the gill lamellae and possible movements.

SEM

For SEM, selected specimens were dehydrated in an increasing series of ethanol (80%, 90% and 99% ethanol, 10 min in each). Subsequently, larvae were critical-point-dried, mounted on holders and sputter-coated with gold-palladium (6 nm). Samples were examined in the scanning electron microscope Hitachi S-4800 SEM (Tokyo, Japan) at an accelerating voltage of 3 kV.

Data analyses

The friction coefficients (μ) of the ventral side of the larvae combined for the different conditions (substrates, weights, before and after removal of the gill lamellae) were tested for normal distribution (Anderson-Darling Normality test) and equal variances (Levene's test). As premises were fulfilled (normally distributed and homogeneous variances) the paired *t*-test was applied because the same larvae were tested under different conditions.
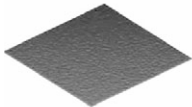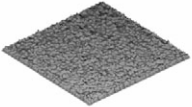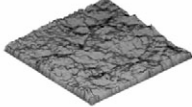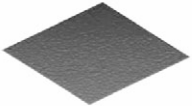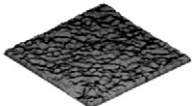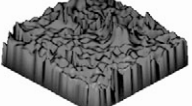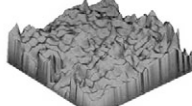
RESULTS
Surface structure of the substrates

Roughness parameters and 3-D profiles reflect the different surface topography of the four investigated substrates. Roughness measurements at lower magnification show increasing values of the roughness parameters R_a and R_z for the substrates S2–S4 (Table 1). Both roughness parameters determined for S2–S4 were in the range of the natural roughness of stream stones. Measurement of the surface topography of S1 was not possible at a lower magnification setting. However, 3-D profiles and low roughness, obtained at the setting of higher magnification as well as SEM pictures (Fig. 4), demonstrated the smoothness of S1.

The roughness parameters evaluated at higher magnification increased for the substrates S1–S3 whereas substrate S4 had roughness parameters almost similar to that of S3. SEM pictures showed the roughness of S4 to be much coarser than that of S3. Moreover, the shape of the texture was very different in both substrates. The roughness of the investigated substrates S2–S4 measured at higher magnification was approximately in the range

Table 1. Parameters of surface roughness (means ± s.d., N=10) and 3-D profile of the tested substrates (S1–S4) at two different magnifications

Substratum	S1	S2	S3	S4
(A) Roughness at lower magnification				
3-D profile area: 1 mm × 1 mm z-range: 1 mm	Measurement not possible			
$R_{a(\lambda=167\,\mu m)}$	–	0.56±0.03 μm	3.33±0.09 μm	6.25±0.23 μm
$R_{z(\lambda=167\,\mu m)}$	–	5.65±0.72 μm	36.03±1.30 μm	59.50±3.53 μm
(B) Roughness at higher magnification				
3-D profile area: 100 μm × 100 μm z-range: 100 μm				
$R_{a(\lambda=16.7\,\mu m)}$	0.05±0.01 μm	0.33±0.02 μm	2.18±0.30 μm	2.19±0.52 μm
$R_{z(\lambda=16.7\,\mu m)}$	0.55±0.18 μm	2.86±0.23 μm	34.61±8.47 μm	32.90±13.29 μm

R_a, arithmetic roughness mean; R_z, mean maximum height of the profile.

of the common natural roughness of stones found in running waters (P.D.-K., unpublished).

Friction properties of the ventral body side

Friction properties of the ventral side of *E. assimilis* larvae were different on the investigated substrates. The lowest values were measured on S3 and the highest ones on S4 and S2 (Fig. 5). With increasing normal force, the friction force increased on all substrates (Fig. 5A–C). The friction coefficient decreased with an increasing normal force (Fig. 5D–F). Besides the real friction force the drag of the larval preparation and the glass plate contributed to the measured values. However, due to the very low velocity of $100\,\mu m\,s^{-1}$ it can be estimated that drag must be lower than $10^{-6}\,mN$ and therefore can be neglected. Moreover, the error caused by drag must be the same for all measurements so that a relative comparison is possible in any case. Differences between substrata S2 *versus* S3, and S3 *versus* S4 were significant for all loads (Table 2). The highest frictional coefficient was determined for the lowest normal forces on all substrata (Fig. 6). It decreased significantly with an added weight (S2, S3, S4; Table 3). Between one and two added weights, there was no difference in frictional coefficient for S1, S3 and S4 substrates. Only on S2 was there a slight but significant (consider

paired test design) decrease of the friction coefficient after adding the second weight.

Effects of gill lamellae on friction in a posterior direction

A significant contribution of the gill lamellae to the friction coefficient was found on three (S1, S2 and S4) of four tested substrates (Table 4) when pulling the larval preparation in the direction of flow (natural direction). The contribution was highest on S2 and almost the same on S1 and S4 (Fig. 7A). Only S3 showed no change of the friction coefficient after removing gill lamellae. The contribution of gill lamellae to the friction was determined by calculating the difference of friction force (ΔF) (or friction coefficient $\Delta\mu$) measured in larvae with and without gill lamellae pulled in a posterior direction.

The friction coefficient ($\mu=F_{friction}/F_{normal}$) allows comparison of the friction at different normal forces. Due to the individuality of samples, normal forces were determined for each single preparation. The reduction of the friction coefficient after removing gill lamellae was 18% on average on S1, 23% on S2 and 15% on S4 for lowest normal force. The contribution of gill lamellae was significant on the substrates S1, S2 and S4 for all weights whereas no difference was found on S3 (Table 4). The reduction of the friction coefficient

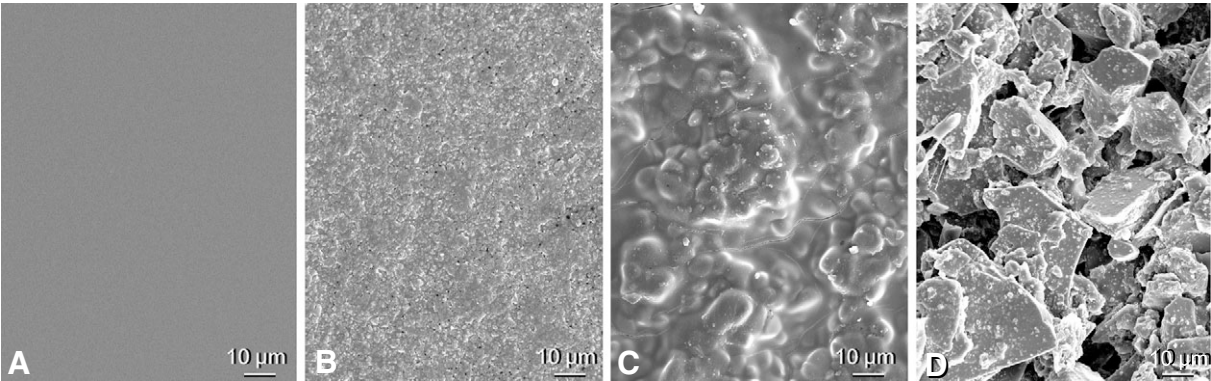
Fig. 4. Investigated substrates: (A) smooth glass, substrate S1, (B) replications of polishing papers with a nominal asperity size of 1 μm, substrate S2, (C) replications of polishing papers with a nominal asperity size of 12 μm, substrate S3, (D) replications of normal polishing papers 400, substrate S4.
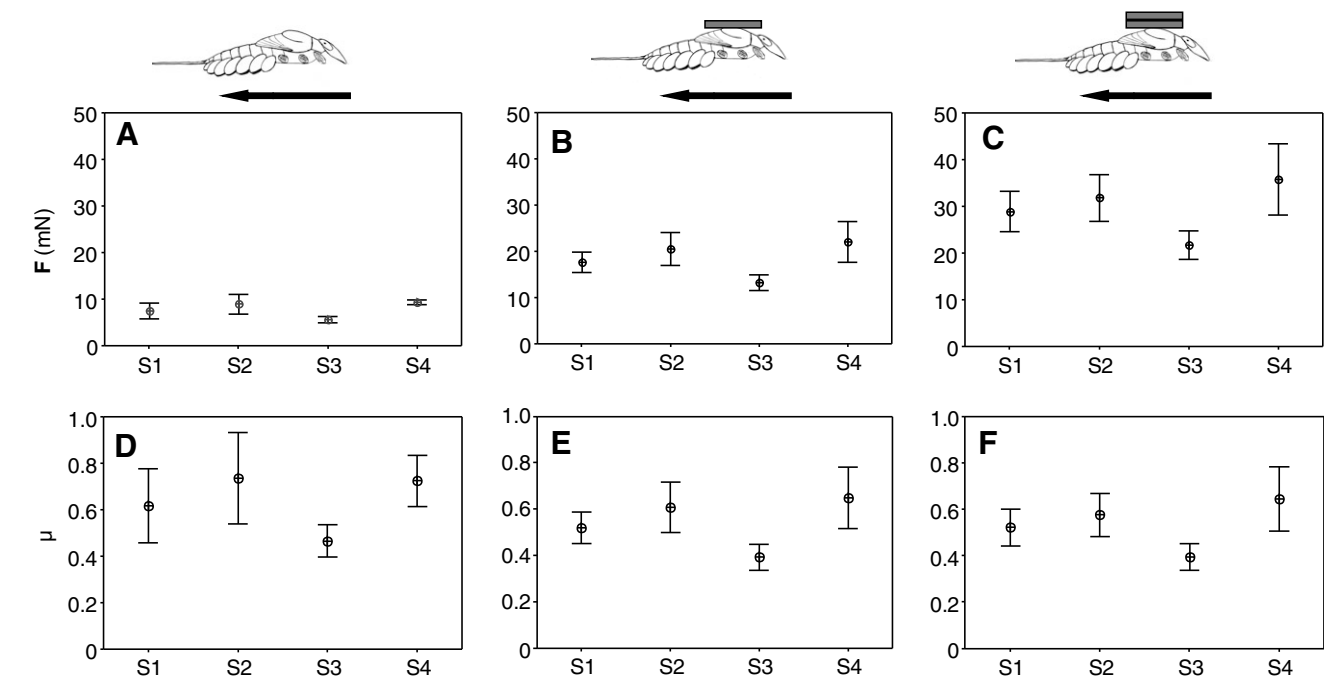
Fig. 5. Friction force F (A–C) and friction coefficient μ (D–F) of the ventral surface of *Epeorus assimilis* measured on four different substrates under different normal forces: (A,D) without added weight – normal force 11.9–12.6 mN, (B,E) with one added weight – normal force 33.5–34.1 mN, (C,F) with two added weights – normal force 55.1–55.8 mN. Bars are 95% confidence intervals for means. Abbreviations: S1–S4, substrates.

with an increasing normal force was 17% on average on S1, 17% on S2 and 15% on S4.

The difference in the frictional force was 1.29±0.90 on S1, 2.10±1.03 on S2, 0.22±0.41 on S3 and 1.29±0.55 on S4 (means ± s.d., N=5) at the lowest weight (W1). The difference in the frictional force increased with increasing normal force. The friction force was up to four times higher after adding two weights (W3) than for W1 (W3: 4.82±2.46 on S1, 5.38±1.20 on S2, 0.01±1.75 on S3 and 5.39±3.66 on S4, means ± s.d., N=5).

Effects of gill lamella on friction in an anterior direction

When the larvae were pulled in an anterior direction, the difference of friction force and friction coefficient (ΔF and $\Delta\mu$) were highest on S1 (Fig. 7D–F). Both values were in the same range similar to the data obtained from pulling in a posterior direction so that no directionality was found on S1. While $\Delta\mu$ showed no significant differences between anterior and posterior pull on S1, $\Delta\mu$ measured in an anterior direction on S2 and S4 was lower than that measured in a posterior direction.

Table 2. Results of the paired *t*-test for friction coefficient of larvae on different substrates (S1–S4)

Comparison	d.f.	t	P
Friction coefficient			
W1			
S1 *vs* S2	4	2.67	0.056
S2 *vs* S3	4	4.99	0.008
S3 *vs* S4	4	5.48	0.005
W2			
S1 *vs* S2	4	3.12	0.036
S2 *vs* S3	4	7.90	0.001
S3 *vs* S4	4	5.75	0.005
W3			
S1 *vs* S2	4	2.08	0.106
S2 *vs* S3	4	8.34	0.001
S3 *vs* S4	4	5.93	0.004

W1, without added weight; W2, with one added weight; W3, with two added weights; S1–S4, substrates; d.f., degrees of freedom; *t*, *t*-value; *P*, probability value.

Table 3. Results of the paired *t*-test for friction coefficient on ventral side in larvae for different normal forces

Comparison	d.f.	t	P
Friction coefficient on S1			
W1 *vs* W2	4	2.68	0.057
W1 *vs* W3	4	3.06	0.038
W2 *vs* W3	4	0.09	0.929
Friction coefficient on S2			
W1 *vs* W2	4	4.02	0.016
W1 *vs* W3	4	4.26	0.013
W2 *vs* W3	4	5.26	0.006
Friction coefficient on S3			
W1 *vs* W2	4	9.47	0.001
W1 *vs* W3	4	5.15	0.001
W2 *vs* W3	4	0.10	0.913
Friction coefficient on S4			
W1 *vs* W2	4	2.97	0.041
W1 *vs* W3	4	2.67	0.056
W2 *vs* W3	4	0.93	0.406

W1, without added weight; W2, with one added weight; W3, with two added weights; d.f., degrees of freedom; *t*, *t*-value; *P*, probability value.
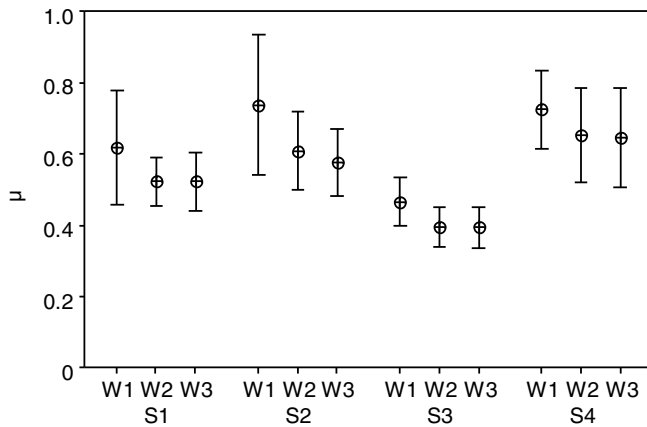
Fig. 6. Friction coefficient (μ) of the ventral surface of *Epeorus assimilis* measured under different normal forces: without added weight (W1), with one added weight (W2), with two added weights. Bars are 95% confidence interval for means. Abbreviations: S1–S4, substrates.

However, Δμ on S2 and S4 was significant only for some tested normal forces while it was in the range of consideration for others (Table 5). On S3, differences in Δμ between both directions of pull were not significant, which means that no contribution of the gill lamellae was found in either direction. The described effects were found more or less clearly for all normal forces (W1–W3).

Morphology of setose pads on gill lamellae

Investigations of gill lamellae in SEM showed that the setae on the pads had different shapes (Fig. 8A). Four different types of setae were distinguished. The largest part of the pad was covered by type 2 setae (ST2). The base of each seta was just slightly tilted whereas the setal tip was bent (Fig. 8B,D,E,H). ST2 were 21.3±1.7 μm long (mean ± s.d., *N*=15). The tip was mostly more or less oriented in a posterior direction. On the anterior–proximal edge, type 1 setae (ST1) were found. These setae were 18.3±1.8 μm long (mean ± s.d.,

N=8) with a compressed tip and were strongly bent at the base (Fig. 8C). The third type of setae (ST3) was located on the lateral–distal edge of the pad. In contrast to the previous setal types, these setae had sharp tips and were hook-shaped (Fig. 8F,G). Moreover, setal tips of ST3 type of setae were oriented more or less in the proximal direction. Distally, the pads bore long setae (ST4), which were surrounding the ST2 and ST3 (Fig. 8A,F). The latter setae were located exactly on this part of the gill lamella, which was not covered by the anterior overlapping gill plate (Fig. 8A). All setae arose from the ventral cuticle of the gill lamella (Fig. 8H,I) and were hollow, at least at their base. Between setae, smaller hair sensilla were found (Fig. 8E).

Mobility of gill lamellae

We succeeded in recording the movements of two single gill lamellae from the ventral side. Videos were recorded through a Plexiglas plate inside of the flume. Movements of the lamellae can clearly be seen in the video. In order to measure these movements, the angle of the deflection of a lamella relative to the corresponding abdominal segment was determined from single video frames (Fig. 9). The angle of the fourth gill lamella changed about 15 deg. within 0.64 s. After a time period of 1.72 s, also the third lamella moved 17 deg. within 0.16 s. The video showed that, in both cases, the contact of the gill lamellae setose pads with the support was broken.

DISCUSSION

Our measurements of the friction force showed, for the first time, that the setose pads on the gill lamellae make a significant contribution to attachment on different substrates. The friction coefficient of the gill lamellae depended on the surface roughness of the substrate and on the pulling direction. Our results show that interlocking effects are mainly responsible for friction generation on the rough substrates whereas molecular interactions (adhesion) seem to contribute to friction on smooth substrates. However, the contribution of the gill lamellae to the friction coefficient in our experiment was lower than expected. Possible reasons are the lack

Table 4. Results of the paired *t*-test for friction coefficient on ventral side in larvae with and without gill lamellae – pull in a posterior direction

Comparison	d.f.	t	P
With GL *vs* without GL			
W1			
S1	4	3.20	0.033
S2	4	4.48	0.011
S3	4	1.27	0.297
S4	4	5.61	0.005
W2			
S1	4	5.80	0.004
S2	4	6.79	0.002
S3	4	0.11	0.917
S4	4	4.22	0.013
W3			
S1	4	4.39	0.012
S2	4	10.00	0.001
S3	4	0.02	0.986
S4	4	3.38	0.028

GL, gill lamellae; W1, without added weight; W2, with one added weight; W3, with two added weights; S1–S4, substrates; d.f., degrees of freedom; *t*, *t*-value; *P*, probability value.

Table 5. Results of the paired *t*-test for friction coefficient of ventral body side in larvae with and without gill lamellae

Comparison	d.f.	t	P
Δμ posterior pull *vs* Δμ anterior pull			
W1			
S1	4	0.92	0.408
S2	4	2.53	0.065
S3	4	0.44	0.686
S4	4	2.69	0.052
W2			
S1	4	0.09	0.932
S2	4	3.98	0.016
S3	4	0.12	0.912
S4	4	3.00	0.040
W3			
S1	4	0.29	0.783
S2	4	3.68	0.021
S3	4	0.70	0.524
S4	4	2.62	0.059

W1, without added weight; W2, with one added weight; W3, with two added weights; S1–S4, substrates; d.f., degrees of freedom; *t*, *t*-value; *P*, probability value; Δμ, difference in friction coefficient.
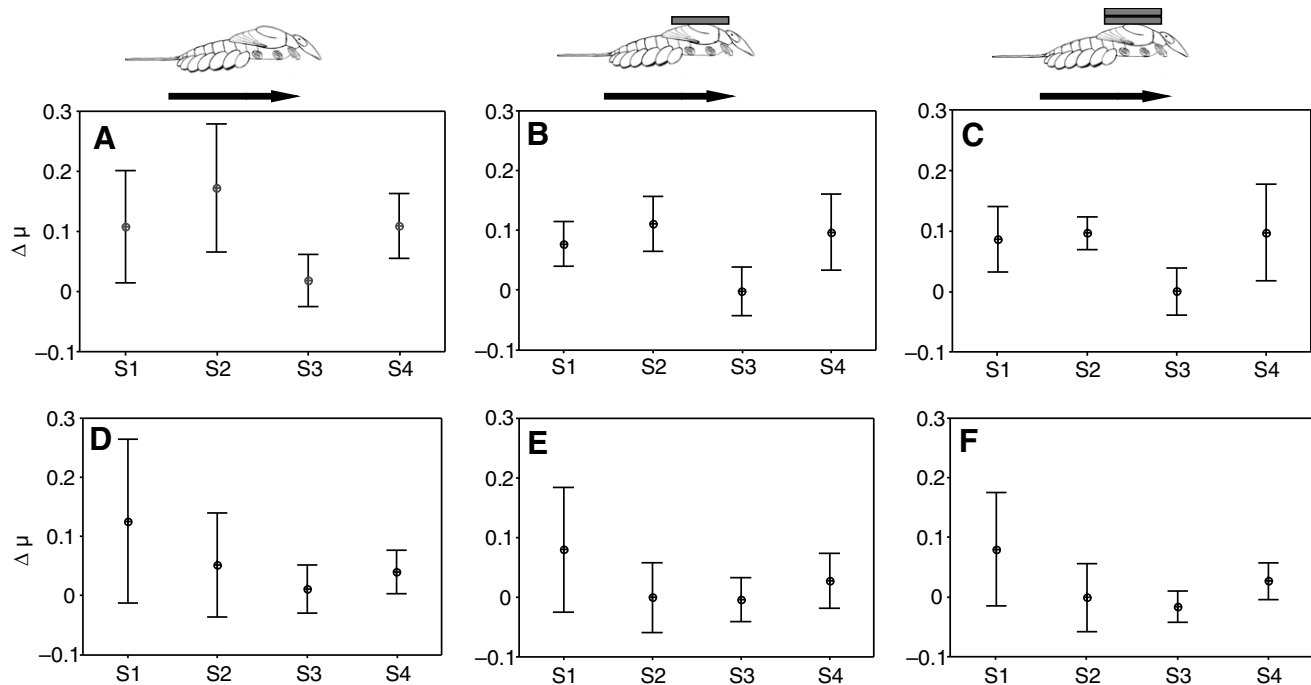
Fig. 7. Effect of the gill lamellae of *Epeorus assimilis* on the friction coefficient μ. Graphs show differences between the friction coefficients in larvae with and without gill lamellae. Larvae pulled in posterior (A–C) and anterior (D–F) direction: without added weights (A,D), with one added weight (B,E) and with two added weights (C,F). Bars are 95% confidence intervals for means. Abbreviations: S1–S4, substrates.

of the active control of body positioning by the larva and changes in material properties of the cuticle due to the dehydration/rehydration. Both factors can cause less than perfect contact formation between the setose pads and the substrate than that under natural conditions. We will discuss these aspects in detail.

Mobility of the gill lamellae
In spite of the previously accepted statement that the gill lamellae in *Epeorus* species are immobile (Ambühl, 1959; Baeumer et al., 2000), our videos of the ventral side of the larvae revealed that the gill lamellae are at least slightly moveable. The ability to move gill lamellae is also supported by the observed presence of two muscles inserted on the gill lamellae of *E. assimilis* (S.N.G. and P.D.-K., personal observation). Species from the closely related genus *Ecdyonurus* are well known for beating with the gill lamellae (Eastham, 1936). *Ecdyonurus* starts gill beating as a respiratory adaptation at moderate hypoxia (Baeumer et al., 2000). This mechanism is not known from *E. assimilis* larvae, which live in swift-running and well-aerated water (Baeumer et al., 2000). It has been described that the gill lamellae of *Epeorus* are immovably spread on the sides and pressed by their costal margins to the substrates (Kluge, 2004). Kluge also mentions that some rheophilous larvae, which are not able to perform fast rhythmic fluctuations, are able to perform slow movements. The observed movements in *E. assimilis* have very low amplitude and are hardly visible to the naked eye. Nevertheless, the movements can be very important for positioning of lamellae during attachment and detachment. Our video recordings show that the lamellae move in a posterior direction and detach themselves from the substrate. Shortly afterwards, the detached larva starts walking. Consequently, the slight movement of the gill lamellae might be important for detachment. It can be assumed that slight movements of the gill lamellae can also create a better adaptation to the support if needed.

Surface roughness and friction
A considerable contribution to friction by the gill lamellae was measured on the smooth substrate (S1) and on some rough substrates (S2, S4) as well. On rough substrates a significant effect of the lamellae was detected only on substrates of a slight roughness (S2) or of a strong roughness (S4). Interestingly, the gill lamellae showed no effect on friction on the substrate with an intermediate roughness (S3). The highest contribution of the gill lamellae to friction was found on S2. On the rough substrates, setae may interlock with surface asperities but the ability to attach to smooth glass (S1) leads us to assume that this cannot be the only attachment mechanism.

On the smooth substrate, the setae with compressed tips (ST1 and ST2) may increase the area of real contact with the substrate and might therefore increase the contribution of molecular forces (adhesion). The spaces between the setae might cause water to escape from the contact regions between setal tips and substrate and thus contribute to the formation of solid–solid intimate contacts responsible for the generation of molecular forces.

On the substrate S2, additional interlocking effects with surface irregularities might be assumed to explain the increased friction force compared with that measured on the smooth substrate (Fig. 10). On the substrate with the coarsest roughness (S4), two different mechanisms might contribute to friction. The setae may interlock with the surface irregularities of the fine scale of roughness (much smaller than the seta size) similar to the effects detected on the substrate S2. Additionally, there could be an interlocking between entire setae and surface irregularities approximately in the range of the seta size. However, due to the shape of the substrate having relatively deep grooves not all setae may have contact to the substrate. It was surprising to see almost no contribution of the gill lamellae to friction on the substrate with an intermediate roughness (S3). We assume that the rounded shape of the substrate tips might offer only a few possibilities for the setae to interlock. Moreover,
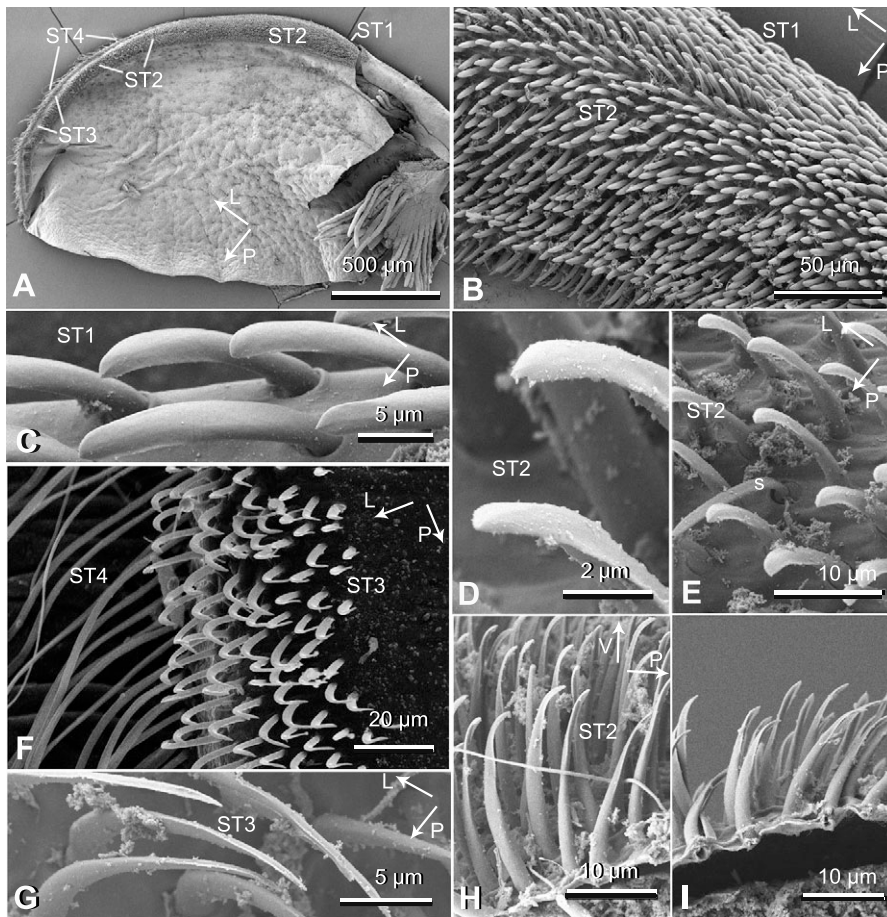
Fig. 8. Setose pads of gill lamellae consisting of different types of setae. (A) Overview of a whole gill lamella, (B) antero-proximal part of the pad with ST1 and ST2, (C) ST1 are compressed and strongly bent at the base, (D,E) ST2 are bent on the compressed tip and only slightly bent at the base, they are the major setal type, (F) latero-distal part of the pad with ST3 and ST4, long hairs, (G) ST3 have a hooked shape with a sharp tip, (H, I) section through a setose pad on a gill lamella, Abbreviations: ST1, type 1 setae; ST2, type 2 setae; ST3, type 3 setae; ST4, type 4 setae; P, posterior; L, lateral; V, ventral; s, sensilla.

due to the configuration of the grooves, too few setae have contact with the substrate (Fig. 4C) to make a significant contribution to friction. Internally, the gill lamellae are filled with liquid and, therefore, in combination with a thin cuticle are able to adapt to the coarse roughness (or waviness) of the substrate. Additionally, the setae with their sharp tips (ST3) may contribute to interlocking with rough substrates. Such interlocking devices on the gill lamellae of *Epeorus sp.* from the Himalaya were labelled as 'spinous pads' which were assumed to be marvelous friction devices (Hora, 1930). Our results support his conclusions, especially for rough substrates.

Furthermore, it has to be taken into account that the functioning of setose pads might work in combination with the other attachment structures. In a former study we assumed that different attachment structures of *E. assimilis* might provide an advantage for larvae in attachment to substrates with different surface properties (Ditsche-Kuru and Koop, 2009). There could be an overlapping range of surface properties for different attachment devices specialised to attachment on particular substrates. For example, insect claws are adapted for interlocking with rather coarse surface roughness only (Dai et al., 2002) whereas the gill lamellae increase friction force not only on rough but also on smooth substrates as well as on substrates with slight surface roughness. The ability of the gill lamella surfaces to attach to smooth surfaces is in agreement with the described ability of larvae to attach to smooth glass (Ambühl, 1959). However, the natural substrates of *Epeorus* larvae are stones, and even smooth stones usually have some small irregularities that provide a grip for the claw. So under natural conditions, even on smooth surfaces, the effect of the gill lamellae may supplement the
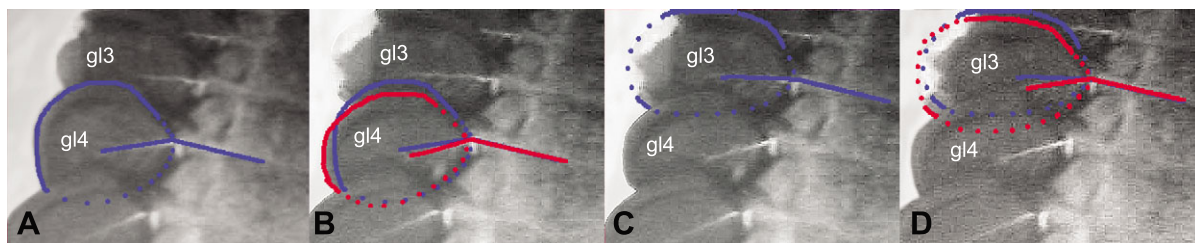

Fig. 9. Separate movements of two gill lamellae of *Epeorus assimilis* recorded by means of videoscope IPLEX II (Olympus), ventral view through a Plexiglas plate in a flume: (A) 0.0 s: position of the gill lamellae before movement, (B) 0.64 s: gill lamella 4 has moved, the angle changed 15 deg., (C) 2.36 s: gill lamellae 3 and 4 in almost the same position as in B, (D) 2.52 s: after gill lamella 3 has moved, the angle changed 17 deg. The position of the gill lamellae before movement is marked in blue, after movement in red. Abbreviation: gl, gill lamella.
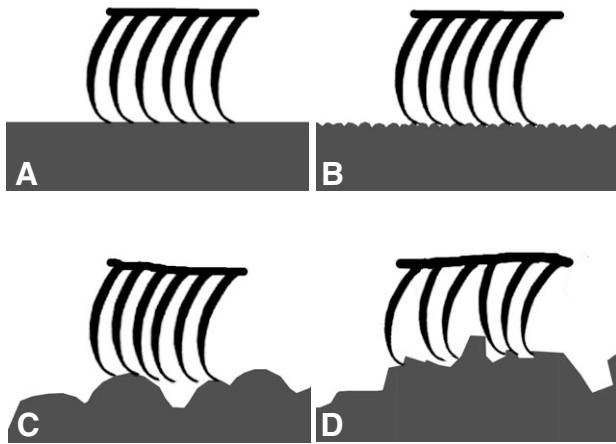
Fig. 10. Diagram of the hypothetical interactions between setae (ST2) and tested substrates: (A) on a smooth surface (S1 substrate) all setal tips are in contact with the support, (B) on the slight roughness of the S2 substrate setal tips remain in contact with the substrate and may interlock with substrate irregularities, (C) on the increased roughness of the S3 substrate with a deeply-grooved microtopography, only a few setae may have intimate contact with the substrate, (D) on the increased roughness of the S4 substrate, setae interlock with surface irregularities.

attachment of the claws. This contribution of the gill lamellae to friction force on smooth substrates might be an advantage for *Epeorus* especially in higher currents, when the larvae have to cope with higher flow forces. In connection with this it is interesting that a significantly higher abundance for *Epeorus* species on smooth substrates compared with rough ones was described (Clifford et al., 1989). The opposite distribution in relation to the surface roughness was observed in the same study for most other species.

However, rather high friction on smooth substrates might be a side effect. Stones, under natural conditions under water, are normally not totally smooth but rather covered with algae and biofilm. Biofilms in running waters usually have a smooth and slippery surface. One may hypothesise that the setose pads of the gill lamellae represent an adaptation to attachment on biofilms. An example of using biofilm for attachment can be found in plants that inhabit waterfalls. Different Podosteamaceae species develop adhesive hairs that stick to cyanobacteria threads and biofilm matrix (Jäger-Zürn and Grubert, 2000). In their habitats, these plants withstand enormous tensile stress caused by the action of running water.

Pulling direction and friction

Most cuticular structures described in this work are directed in a posterior direction, and directionality in friction was found on rough substrates while on smooth substrates no directionality was shown. On the rough substrates (S2, S4), the gill lamellae contributed to friction in the direction of the shear force (posterior) caused by water current, while in an anterior direction such a contribution was less expressed. This can be explained by the interlocking of the setae located on gill lamellae with the surface irregularities. However, on both substrates still some small positive effects of the gill lamellae on friction are found.

Drag forces caused by water current and friction

The mean friction force of the larval preparation without additional weight was between 5.6 mN and 9.4 mN for different substrates.

The friction of the larvae has to withstand the drag force caused by flow. It has to be taken into account that in living insects the claws also contribute to friction. Moreover, the friction force is influenced by normal force. Consequently, a comparison with the values measured on living larvae is difficult. Nevertheless, the measured friction force of the whole ventral side (without claws) exceeds the drag forces as determined on living *E. assimilis* larvae. The highest measured drag forces were about 4.5 mN for living larvae (Weißenberger et al., 1991), which however is not the maximum drag. Drag increases with flow velocity and in the experiments of Weißenberger et al. larvae had no problems remaining attached to the substrate (Weißenberger et al., 1991). So higher drag forces have to be expected at higher flow velocities.

Conclusions

Our results revealed that the pads significantly contributed to friction force generated on smooth and on some rough substrates but not on certain surfaces of intermediate roughness. The contribution of pads to the friction coefficient in experiments was lower than expected under natural conditions, which may be caused by a smaller contact area between the pads and the substrate (changes in material properties, lack of the active control of body positioning of the larva). The friction coefficient of the gill lamellae with the substrate depended on the surface roughness of the substrate and on the pulling direction. These results suggest that interlocking between structures of the insect cuticle and substrate irregularities as well as molecular adhesion contribute to friction.

LIST OF ABBREVIATIONS

F	friction force
F_{normal}	normal force
R_a	arithmetic roughness mean
R_z	mean maximum height of the profile
S1–S4	substrate types
SEM	scanning electron microscopy
ST1–4	setal types
W1–W3	three ranges of normal forces applied in experiments
ΔF	difference of friction force in larvae with and without gill lamellae
$\Delta\mu$	difference of friction coefficients in larvae with and without gill lamellae
λ_c	cutoff length
μ	friction coefficient

REFERENCES

Ambühl, H. (1959). Die Bedeutung der Strömung als ökologischer Faktor. *Schw. Z. Hydrol.* **21**, 133-264.
Autumn, K. (2006). Properties, principles, and parameters of gecko adhesive system. In *Biological Adhesives* (eds A. M. Smith and J. A. Callow), pp. 225-255. Berlin: Springer.
Autumn, K., Liang, Y. A., Hsieh, S. T., Zesch, W., Kenny, T. W., Fearing, R. and Full, R. J. (2000). Adhesive force of a single gecko foot-hair. *Nature* **405**, 681-685.
Baeumer, C., Pirow, R. and Paul, R. J. (2000). Respiratory adaptations to running-water microhabitats in mayfly larvae *Epeorus sylvicola* and *Ecdyonurus torrentis*, Ephemeroptera. *Physiol. Bioch. Zool.* **73**, 77-85.
Bauernfeind, E. and Humpesch, U. H. (2001). *Die Eintagsfliegen Zentraleuropas (Insecta: Ephemeroptera): Bestimmung und Ökologie*, Wien: AV-Druck.
Clifford, H. F., Gotceitas, V. and Casey, R. J. (1989). Roughness and color of artificial substratum particles as possible factors in colonization of stream invertebrates. *Hydrobiologia* **175**, 89-95.

Dai, Z., Gorb, S. N. and Schwarz, U. (2002). Roughness dependent friction force of the tarsal claw system in the beetle *Pachnoda marginata* (Coleoptera, Scarabaedae). *J. Exp. Biol.* **205**, 2479-2488.

DIN ISO 6344 (2000). *Schleifmittel auf Unterlagen - Korngrößenanalyse - Teile 1-3.* Berlin, Wien, Zürich: Beuth Verlag.

Ditsche-Kuru, P. and Koop, J. H. E. (2009). New insights into a life in current: do the gill lamellae of *Epeorus assimilis* and *Iron alpicola* larvae (Ephemeroptera: Heptageniidae) function as a sucker or as friction pads? In *International Perspectives in Mayfly and Stonefly Research* (ed. A. H. Staniczek). *Aquat. Insects* **31**, 495-506.

Dodds, G. S. and Hisaw, F. (1924). Ecological studies of aquatic insects. 1. Adaptations of mayfly nymphs to swift streams. *Ecology* **5**, 137-148.

Eastham, L. E. S. (1936). The gill movements of nymphal *Ecdyonurus venosus* (Ephemeroptera) and the currents produced by them in water. *J. Exp. Biol.* **14**, 219-228.

Gonser, T. (1990). Beiträge zur Biologie südneotropischer Ephemeropteren, Dissertation, Albert-Ludwig Universität Freiburg.

Gorb, S. (2001). *Attachment Devices of Insect Cuticle.* Dortrecht: Kluwer Academic Publishers.

Gorb, S. N. and Beutel, R. G. (2001). Evolution of locomotory attachment pads of hexapods. *Naturwissenschaften* **88**, 530-534.

Gorb, S. N., Beutel, R., Gorb, E. V., Jiao, Y., Kastner, V., Niederegger, S., Popov, L. V., Scherge, M., Schwarz, U. and Vötsch, W. (2002). Structural design and biomechanics of friction-based releasable attachment devices in insects. *Integr. Comp. Biol.* **42**, 1127-1139.

Haas, F. and Gorb, S. N. (2004). Evolution of locomotory attachment pads in the Dermaptera (Insecta). *Arthopod Struct. Devl.* **33**, 45-66.

Haybach, A. and Malzacher, P. (2002). Verzeichnis der Eintagsfliegen Deutschlands (Insecta: Ephemeroptera). *Entomol. Z. Stutt.* **112**, 34-45.

Hora, S. L. (1930). Ecology, bionomics and evolution of the torrential fauna, with special reference to the organs of attachment. *Philos. Trans. R. Soc. Lond. B. Biol. Sci.* **218**, 171-282.

Huber, G., Mantz, H., Spolenak, R., Mecke, K., Jacobs, K., Gorb, S. N. and Arzt, E. (2005). Evidence for capillarity contributions to gecko adhesion from single spatula nanomechanical measurements. *Proc. Natl. Acad. Sci. USA* **102**, 16293-16296.

Huber, G., Gorb, S. N., Hosoda, N., Spolenak, R. and Arzt, E. (2007). Influence of surface roughness on gecko adhesion. *Acta Biomater.* **3**, 607-610.

Hynes, H. B. N. (1970). *The Ecology of Running Waters.* Liverpool: Liverpool University Press.

Jäger-Zürn, I. and Grubert, M. (2000). Podostemaceae depend on sticky biofilms with respect to attachment to rocks in waterfalls. *Int. J. Plant Sci.* **161**, 599-607.

Kesel, A. B., Martin, A. and Seidl, T. (2004). Getting a grip on spider attachment: an AFM approach to microstructure adhesion in arthropods. *Smart Mater. Syst.* **13**, 512-518.

Kluge, N. (2004). *The Phylogenetic System of Ephemeroptera.* Dordrecht, Boston, London: Kluwer Academic Publishers.

Langer, M. G., Ruppersberg, J. P. and Gorb, S. N. (2004). Adhesion forces measured at the level of a terminal plate of the fly's seta. *Proc. R. Soc. Lond. B. Biol. Sci.* **271**, 2209-2215.

Minshall, J. N. (1967). Life history and ecology of *Epeorus pleuralis* (Banks) (Ephemeroptera: Heptageniidae). *Am. Midl. Nat.* **78**, 369-388.

Ruttner, F. (1962). *Grundriss der Limnologie.* Berlin: Walter De Gryter and Co.

Staniczek, A. (2003). *Eintagsfliegen-Manna der Flüsse.* Stuttgarter Beiträge zur Naturkunde Ser. C 53.

Statzner, B. and Holm, T. F. (1982). Morphological adaptations of benthic invertebrates – an old question studied by means of a new technique (laser doppler anemometry). *Oecologia* **53**, 290-292.

Stork, N. E. (1980). Experimental analyses of adhesion of *Chrysolina polita* (Chrysomelidae, Coleoptera) on a variety of surfaces. *J. Exp. Biol.* **88**, 91-107.

Volk, R. (2005). *Rauheitsmessungen, Theorie und Praxis* (ed. DIN Deutsches Institut für Normung). Berlin, Wien, Zürich: Beuth Verlag.

Weißenberger, J., Spatz, H. C., Emanns, A. and Schwoerbel, J. (1991). Measurement of lift and drag forces in the mN range experienced by benthic arthropods at flow velocities below 2.1 ms-1. *Freshw. Biol.* **25**, 21-31.

Wellnitz, T. A., Poff, N. L., Cosyleon, G. and Steury, B. (2001). Current velocity and spatial scale as determinants of distribution and abundance of two rheophilic herbivorous insects. *Landscape Ecol.* **16**, 3661-3670.

Wesenberg-Lund, C. (1943). *Biologie der Süßwasserinsekten.* Reprint 1989, Königsstein: Koelz Scientific Books.

Wichard, W., Arens, W. and Eisenbeis, G. (2002). *Biological Atlas of Aquatic Insects.* Stenstrup: Apollo Books.